

Self-Assembly of Hexakis(4-pyridylmethoxy)cyclotriphosphazene and 1,4-Anthracenedicarboxylic Acid: Structure and Inclusion Behavior

Tomoyuki Itaya,* Nagao Azuma,† and Kenzo Inoue*,††

Chemical Laboratory, Nagano National College of Technology, Nagano 381-8550

†Department of Chemistry, Faculty of Science, Ehime University, Matsuyama 790-8577

††Department of Applied Chemistry, Faculty of Engineering, Venture Business Laboratory, Ehime University, Matsuyama 790-8577

(Received April 8, 2002)

2,2,4,4,6,6-Hexakis(4-pyridylmethoxy)-2λ^5,4λ^5,6λ^5,-cyclotriphosphazene (PyPN) and 1,4-anthracenedicarboxylic acid (DCA) formed polymeric supramolecules through hydrogen bonding between carboxyl and pyridyl groups. Two supramolecular self-assemblies were obtained: crystals **1** composed of PyPN/DCA = 1:2 from DMSO solution, and crystals **2** composed of PyPN/DCA = 1:3 from DMF solution. The former is monoclinic, space group $P2_1/n$ with a = 12.419 Å, b = 24.10 Å, c = 20.794 Å, β = 93.53°, V = 6212 Å^3, Z = 4. The X-ray analysis showed that the complementary hydrogen bonding occurs with two DCA molecules, one on each side of the phosphazene ring of PyPN, to give a novel assembly with polymeric structure. The self-assembly obtained from DMF solution seems to take a cylindrical structure composed of an alternating sequence of one PyPN and three DCA molecules and to be packed into a hexagonal arrangement, as suggested by X-ray diffraction data. These results and the inclusion behaviors of the solvent molecules into **1** and **2** are described.

Supramolecular self-assembly is an efficient way to construct novel molecular architectures with potentially useful properties and functions that are absent in the individual components.[1–4] A particular effort is being directed toward the synthesis of nanoporous molecular-based solids that reveal structural and functional similarities to the inorganic zeolites, because the channels of supramolecular porous materials are potentially tunable by choosing the unit size of the building block.[5–8] In the construction of nanoporous materials, not only the structure of supramolecules but also their arrangement in the solid state is the most important key.

Cyclotriphosphazenes, which are prepared through the introduction of organic groups into the P-Cl group in hexachlorocyclotriphosphazene, act as multifunctional compounds since six organo groups are connected in pairs to each P atom of the phosphazene ring.[9,10] Moreover, in 2,2,4,4,6,6-hexaphenoxy-2λ^5,4λ^5,6λ^5-cyclotriphosphazene, the phenoxy groups are located perpendicularly above and below the nearly planar phosphazene ring.[11,12] By utilizing such unique features, we have recently reported that the complementary hydrogen bondings between 2,2,4,4,6,6-hexakis(4-pyridylmethoxy)-2λ^5,4λ^5,6λ^5-cyclotriphosphazene (PyPN) and 2,2,4,4,6,6-hexakis(4-carboxyphenoxy)-2λ^5,4λ^5,6λ^5-cyclotriphosphazene (CPN),[13] between PyPN and terephthalic acid (TPA),[14] between PyPN and 1,4-naphthalenedicarboxylic acid (DCN)[15] give rise to the cylindrical-shaped supramolecules. In addition, the cylindrical assemblies obtained from PyPN and DCN were laterally packed into a hexagonal arrangement and, a tunnel-like void capable of including iodine was created among them. In this study, we chose more bulky 1,4-anthracenedicarboxylic acid (DCA) as the counterpart of PyPN. If the geometrical features of organophosphazenes hold for the supramolecular assembly formed from PyPN and DCA, the assembly would be expected to take a cylindrical structure. In addition, the packing of cylindrical-shaped assemblies containing bulky and rigid anthracene rings seems to afford a void in the crystal.

We report herein the two hydrogen-bonded supramolecules obtained from PyPN and 1,4-anthracenedicarboxylic acid (DCA). The synthetic method, structural features, and inclusion properties of the supramolecules are described.

Experimental

Materials. 2,2,4,4,6,6-Hexakis(4-pyridylmethoxy)-2λ^5,4λ^5,6λ^5-cyclotriphosphazene (PyPN) was synthesized from the reaction of hexachlorocyclotriphosphazene with sodium 4-pyridinemethoxide prepared from 4-pyridinemethanol (Koei Chemical) and NaH in dry THF, as described in the previous paper.[13] 1,4-Anthracenedicarboxylic acid (DCA) was prepared according to a procedure described in the literature.[16] Other reagents were of analytical grade and without further purification.

Preparation of Supramolecules. A typical procedure is as follows. A DMSO solution of PyPN (4.1×10^{-2} g, 5.2×10^{-5} mol) was added into a DMSO solution of DCA (4.0×10^{-2} g, 1.5×10^{-4} mol). The mixture (2 mL) was allowed to stand at room temperature. Prismatic crystals **1** were deposited. Yield, 21%. Anal. Calcd for $C_{68}H_{56}N_9O_{14}P_3$·0.2(DMSO): C, 61.69; H, 4.33; N, 9.46%. Found: C, 60.91; H, 4.30; N, 9.03%. FT-IR: 2450, 1920, 1698, 1610, 1240, 1040 cm^{-1}. Similary, needle crystals **2** were obtained from a DMF solution containing PyPN and DCA.

Table 1. Crystal Data of **1**

Empirical formula:	$C_{68}H_{58}N_9O_{14}P_3$
Formula weight:	1316.17
Crystal system:	monoclinic
Space group:	$P2_1/n$
Lattice parameter:	a = 12.419(3) Å
	b = 24.10(2) Å
	c = 20.794(4) Å
	β = 93.53(2)°
Volume:	6212(5) Å^3
Fomula units/unit cell:	4
d_{calc}:	1.407 g/cm^3
F(000):	2736
Mo $K\alpha$ radiation	λ = 0.71069 Å
μ:	1.65 cm^{-1}
Number of reflections measured:	15283
Observed:	8096
Final R value:	0.086
Goodness of fit:	1.40

Yield, 40%. Anal. Calcd for $C_{84}H_{66}N_9O_{18}P_3$·1.2(DMF): C, 63.00; H, 4.49; N, 8.55%. Found: C, 62.50; H, 4.37; N, 8.14%. FT-IR: 2450, 1920, 1700, 1680, 1610, 1240, 1040 cm^{-1}.

Measurements. Elemental analyses were carried out with a Perkin-Elmer 240C elemental analyzer (Advanced Instrumentation Center for Chemical Analysis, Ehime University). FT-IR spectra were recorded on a JASCO FT-IR 230 spectrophotometer, applying the KBr pelleting technique. Wide angle X-ray diffraction patterns were obtained using Rigaku RINT 2000 system. Fluorescence spectra were recorded on a Shimadzu RF-5000 spectrofluorometer. Differential scanning calorimetry was done using a Shimadzu DSC-50 calorimeter with sealed aluminium pans at a heating rate of 10/min.

X-ray Data, Structure Determination and Refinement. The three-dimensional X-ray data of the prismatic crystal obtained from the DMSO solution were collected by the use of graphite-monochromated Mo $K\alpha$ radiation (λ = 0.71069 Å) on an automated Rigaku AFC-5R diffractometer. Cell constants and an orientation matrix for data collection were obtained from a least-squares refinement using the setting angles of 25 carefully centered reflections in the range of $23.4 < 2\theta < 25.0°$. The intensities were corrected for Lorentz and polarization effects. The crystal structure was solved by the direct method using the MITHRIL program.[17] The coordination and anisotropic thermal parameters for non-hydrogen atoms were refined by using a full matrix least square procedure. The positions of hydrogen atoms were idealized (C–H; 0.95 Å). The intensity data of 8096 independent reflections were collected and 852 data were used in the solution and refinement (R = 0.086). A summary of data collection and refinement parameters are given in Table 1. Crystallographic data have been deposited at the CCDC, 12 Union Road, Cambridge CB2 1EZ, UK and copies can be obtained on request, free of charge, by quoting the publication citation and the deposition number 190287. The date are also deposited sa Document No. 75042 at the Office of the Editor of Bull. Chem. Soc. Jpn.

Results and Discussion

Formation of the Supramolecular Assembly from PyPN and DCA. The self-assembly of PyPN with DCA in DMSO or DMF solution gave brown crystals **1** and **2**, respectively

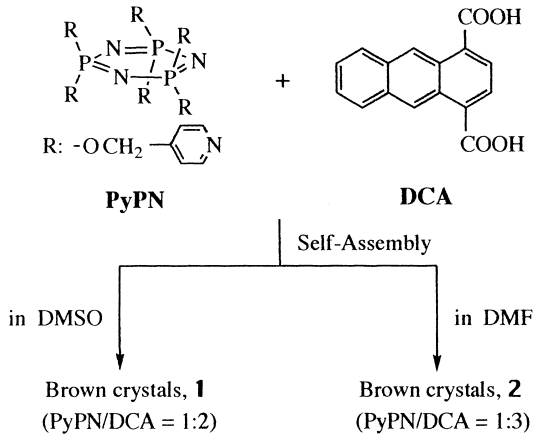

Fig. 1. Formation of the self-assemblies composed of PyPN and DCA.

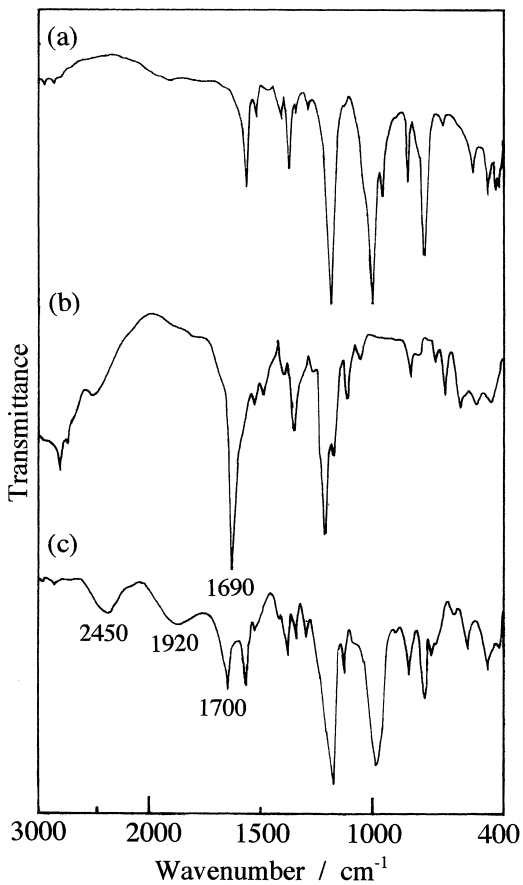

Fig. 2. FT-IR spectra of PyPN (a), DCA (b), and **1** (c).

(Fig. 1). Figure 2 shows the FT-IR spectra of PyPN, DCA, and **1**. Etter[18] has pointed out that the strongest hydrogen bond acceptor binds to the strongest donor, suggesting that carboxylic groups form hydrogen bonds with pyridine units rather than self-association of carboxylic acids. In the FT-IR spectrum of **1**, the broad band of carboxylic acids of DCA at 2600 cm^{-1}–3000 cm^{-1} disappeared and the peaks due to hydrogen bonding between the carboxyl and pyridyl groups appeared at 2450 cm^{-1} and 1920 cm^{-1}, accompanied by the shift of C=O

Table 2. Selected Bond Lengths (Å) and Angles (deg)

P(1)–N(1)	1.576(4)	O(1)–P(1)–O(2)	102.2(3)
P(1)–N(3)	1.564(4)	O(3)–P(2)–O(4)	99.6(2)
P(2)–N(1)	1.581(4)	O(5)–P(3)–O(6)	104.3(2)
P(2)–N(2)	1.572(4)	P(1)–O(1)–C(1)	121.2(4)
P(3)–N(2)	1.574(4)	P(1)–O(2)–C(7)	157.4(6)
P(3)–N(3)	1.577(4)	P(2)–O(3)–C(13)	121.0(3)
P(1)–O(1)	1.560(4)	P(2)–O(4)–C(19)	122.1(4)
P(1)–O(2)	1.532(5)	P(3)–O(5)–C(25)	121.3(4)
P(2)–O(3)	1.578(3)	P(3)–O(6)–C(31)	122.8(3)
P(2)–O(4)	1.578(4)	O(1)–C(1)–C(2)	108.2(5)
P(3)–O(5)	1.573(4)	O(2)–C(7)–C(8)	131.7(8)
P(3)–O(6)	1.569(3)	O(3)–C(13)–C(14)	114.5(4)
P(2)–O(4)	1.578(4)	O(4)–C(19)–C(20)	108.7(5)
O(1)–C(1)	1.442(6)	O(5)–C(25)–C(26)	110.9(5)
O(2)–C(7)	1.055(7)	O(6)–C(31)–C(32)	109.8(4)
O(3)–C(13)	1.443(6)	P(1)–O(1)–C(1)–C(2)	142.9(4)
O(4)–C(19)	1.419(6)	P(1)–O(2)–C(7)–C(8)	11(4)
O(5)–C(25)	1.438(6)	P(2)–O(3)–C(13)–C(14)	103.2(5)
O(6)–C(31)	1.433(6)	P(2)–O(4)–C(19)–C(20)	131.9(5)
		P(3)–O(5)–C(25)–C(26)	−117.7(4)
		P(3)–O(6)–C(31)–C(32)	−127.7(4)

stretching band from 1690 cm^{-1} to 1700 cm^{-1}.[14,15] The single crystal X-ray analysis results indicated that the self-association of carboxylic acids did not exist in **1**, as will be seen later. Rather, these results indicate that PyPN and DCA are linked through the hydrogen bonding between carboxylic acid and pyridyl group.

The elemental analysis of **1** showed that **1** is composed of PyPN/DCA = 1:2, suggesting that not all six pyridyl groups participate in the hydrogen bonding and that two groups are free.

Fortunately, the crystals of **1** grew large enough to conduct single crystal X-ray analysis. The selected bond distances and angles, the arrangement of the assembly in the unit cell and ORTEP diagram of PyPN and DCA are shown in Table 2 and Fig. 3, respectively. The assemblies crystallize in the space group $P2_1/n$ and the unit cell contains eight DCA and four PyPN molecules. The complementary hydrogen bonding occurs with two DCA molecules, one on each side of the phosphazene ring of PyPN, to give a polymeric structure as shown in Scheme 1. The average hydrogen bonded N···HO distance of 2.62 Å is short compared to the sum of the van der Waals radius, 3.20 Å, indicating the formation of strong hydrogen bonding. Interestingly, both pyridyl groups attached to the P3 atom form hydrogen bonds with DCA, whereas one of two groups attached to the P1 and P2 atoms remains without hydrogen bonding. The pyridyl groups that interact with DCA are linked to the phosphazene ring with an average P–O–C bond angle of 121.8°, O–C–C bond angle of 109.4°, and P–O–C–C torsion angle of 130.0°, suggesting that the pyridyl groups are almost located perpendicularly on the phosphazene ring. On the other hand, the free pyridyl groups do not take positions that enable directed interaction with DCA; P–O–C bond angles of 157.4 and 121.0°, O–C–C bond angles of 131.7 and 114.5°, and P–O–C–C torsion angles of 11 and 103.2°. The distance and dihedral angle between the free pyridyl groups and neighboring anthracene ring are about 3.6 Å and 7°, indicative of the occurrence of a π–π interaction between them.

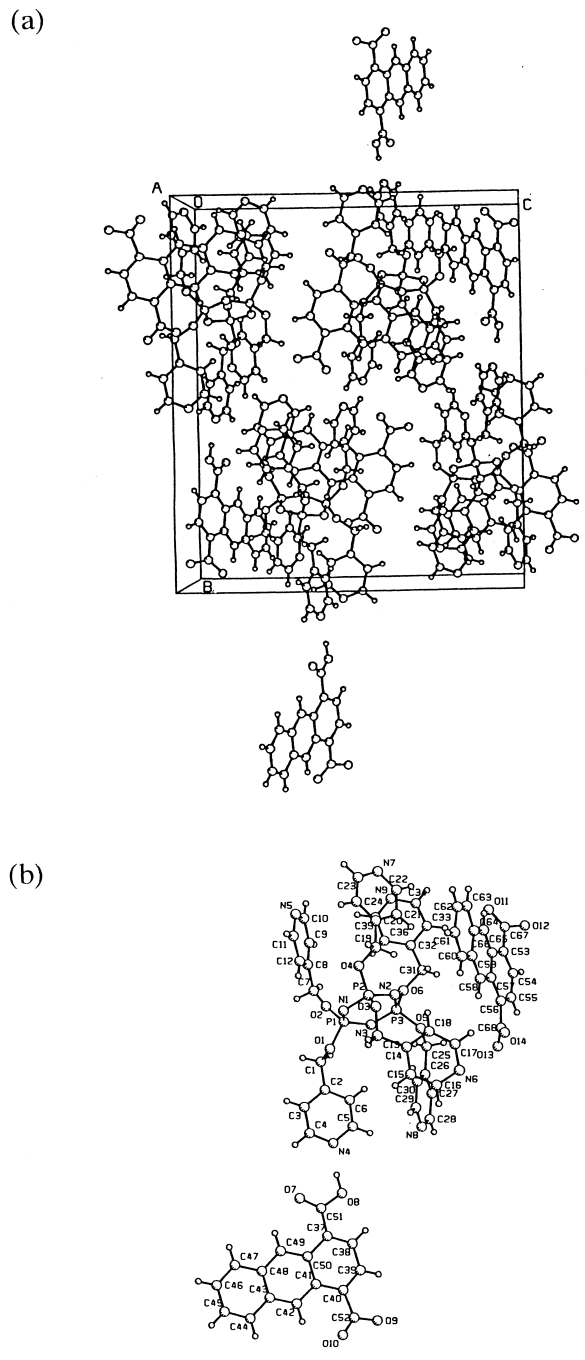

Fig. 3. Arrangement of the assembly **1** in the unit cell and ORTEP diagrams of PyPN and DCA in **1**.

The self-assembly **2** obtained from DMF solution presents a different structure from **1**. From elemental analysis and ^{1}H NMR measurement of **2**, the stoichiometry was found to be PyPN/DCA = 1:3. Again, the disappearance of the band at 2600 cm^{-1}–3000 cm^{-1} assigned to –OH stretching vibration (COOH) and the peaks due to hydrogen bonding between the carboxyl and pyridyl groups at 2450 cm^{-1} and 1920 cm^{-1} were observed for the FT-IR spectrum of **2**. These changes were similar to those of **1**. These results suggest that the hydrogen bonding with an alternating sequence of one PyPN and three

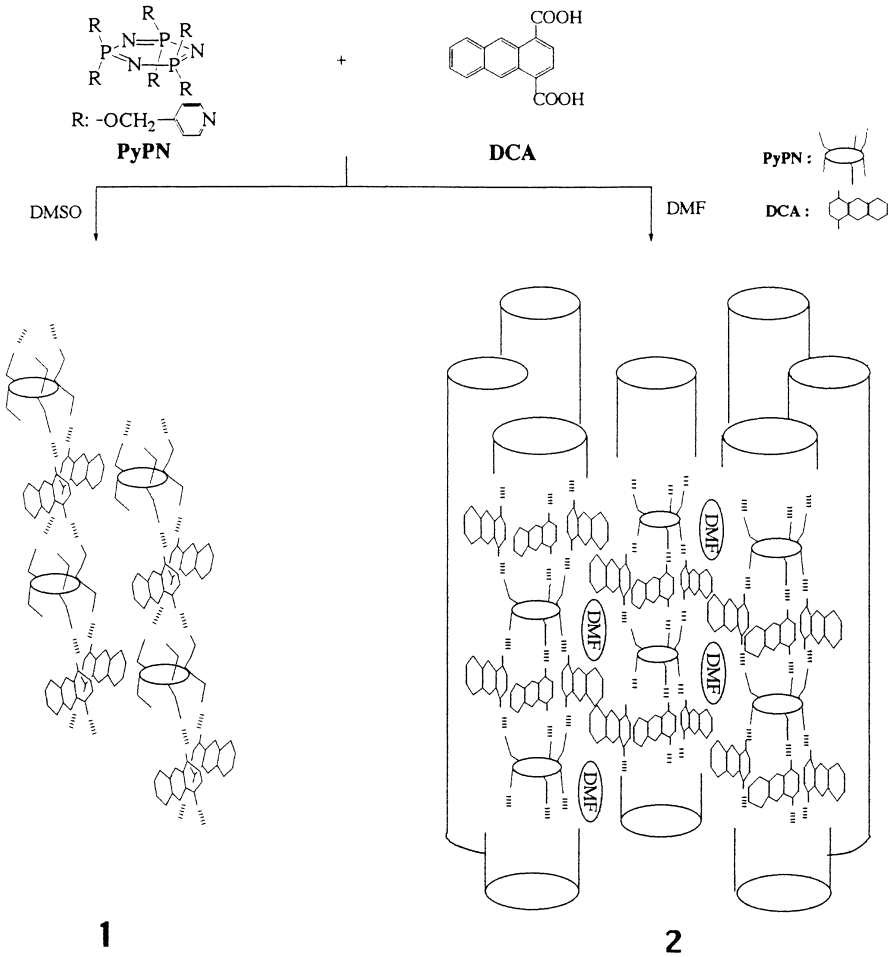

Scheme 1. Schematic representation of structures of **1** and **2**.

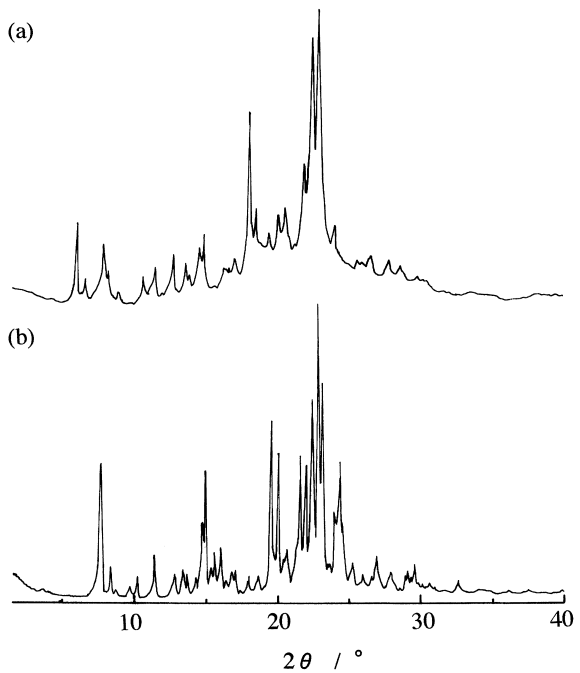

Fig. 4. Comparison of powder X-ray diffraction pattern of **2** with that of the assembly composed of PyPN and 1,4-naphthalenedicarboxylic acid.

DCA molecules gives a polymeric assembly **2** composed of $[PyPN{\cdot}3(DCA)]_n$.

Since the precise molecular structure of **2** have not been ascertained due to difficulties in obtaining single crystals, the structure was examined by X-ray diffraction measurement (Fig. 4 and Fig. 5) and fluorescence spectroscopic method (Fig. 7). The X-ray diffraction pattern observed for **2** was similar to that of the supramolecular assembly of PyPN and 1,4-naphthalenedicarboxylic acid (DCN) (Fig. 4), in which the cylindrical-shaped assemblies are laterally packed into a hexagonal arrangement with the space of 13.3 Å.[15] In the pattern of **2**, in addition, we observed that the diffractions yielded spacing with the 1, $1/\sqrt{3}$, and 1/2 … ratio; the lowest angle peak at d = 14.02 Å, the small peak at d = 8.10 Å, and the very small peak at d = 7.03 Å respectively. These results suggest that the cylindrical-shaped assemblies composed of PyPN and DCA self-organize a hexagonal arrangement with the space of 16.2 Å ($= 14.02 \times 2/\sqrt{3}$) (Fig. 6). As will be seen later, solvent DMF molecules were included into the assembly crystals of **2**. On the other hand, the inclusion behavior was not observed for the assembly composed of PyPN and DCN. These results indicate that the anthracene rings with bulkiness lead to more enlarging of the space among cylindrical-shaped assemblies **2** than do the naphthalene rings.[15]

The geometrical arrangement of anthracene rings of DCA in

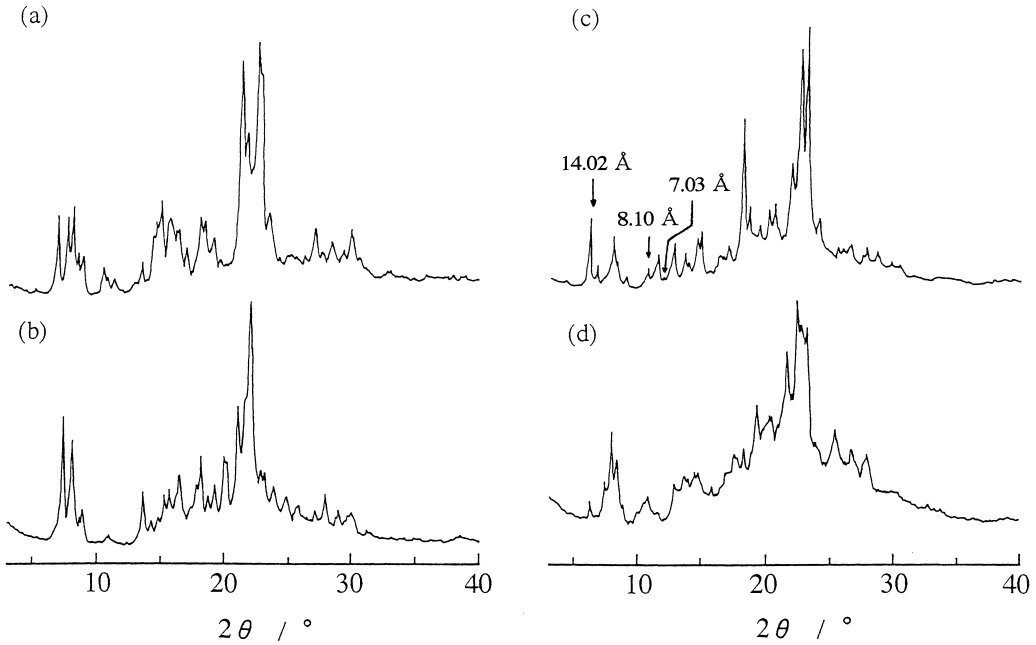

Fig. 5. Powder X-ray diffraction patterns of **1** (a) and **2** (b): (up) the original crystal; (down) the solid prepared by slow cooling after heating to 150 °C.

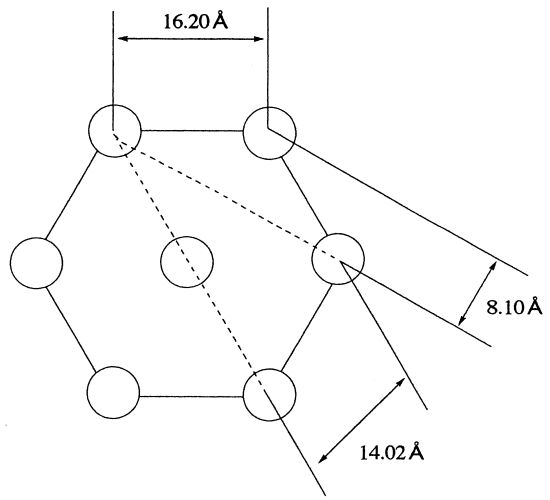

Fig. 6. Schematic representation of a possible hexagonal packing for **2**.

the assembly crystal may be reflected in the fluorescence spectra. The solid-state fluorescence spectra of **1** and **2** are shown in Fig. 7. The spectrum of **1** showed a excimer peaked at 540 nm together with monomeric emission of the anthracene ring. As shown in Fig. 3, the anthracene rings are in close proximity, but do not overlap each other in the crystal of **1**. On the other hand, the fluorescence spectrum of **2** consists of almost all excimer emission with peak wavelength about 580 nm. It is reported that the crystal of anthraceno-crown ether complexed with Na^+ exhibited a fluorescence with λ_{max} = 580 nm, where the two anthracene rings are aligned, forming a slightly staggered sandwich with an inter planar distance of ca. 3.4 Å.[19] From these results, one can conclude that pairs of the anthracene rings stacked over each other exist in the crystal of **2**.

Thus, the process of assembly from PyPN and DCA was affected by the solvents. The hydrogen bonding between PyPN and DCA and the packing of assemblies in the crystal may be the key to determine the structure of the assembly. The carboxyl groups of DCA are solvated with DMF and DMSO, but the interaction between the carboxyl groups and these solvents is significantly different, i.e., DMSO interacts strongly with the carboxyl group, compared to DMF. The loosely solvated DCA with DMF could exchange hydrogen bonding acceptors (pyridyl groups) to form triple hydrogen bonds. It seems likely that this difference affects the stoichiometry of the assembly.

Inclusion of Solvent Molecule into the Assembly Crystal. As the assemblies contain rigid and bulky anthracene rings, the assemblies with cylindrical structure are difficult to pack together in a space-saving arrangement. Especially, when the assemblies **2** are packed together in the hexagonal arrangement, substantial voids seem to appear along the assemblies in the crystal of **2**. If so, the solvent molecules used for assembly formation may be included into the spaces among the assemblies.

Figure 8 shows the ^{1}H NMR spectra of **1** (in DMF-d_7) and **2** (in DMSO-d_6). The samples were repeatedly washed with ether. In the spectra of **1** and **2**, not only the signals for PyPN and DCA but also the signals for the DMSO and DMF molecules were observed, respectively, indicating that the solvent molecules partially fill the void in the assembly crystals. From the integral ratio, the numbers (per repeated unit of assemblies) of the DMF molecules included into **2** are estimated to be 1.2, which is agreement with the elemental analysis data. On the other hand, the number of the DMSO molecules included into **1** was approximately a tenth of that of the DMF molecules included into **2**. These results suggest that **2** forms a more suitable void for inclusion of the solvent molecules in the crystal than does **1**. The hexagonal packing of the cylindrical-shaped

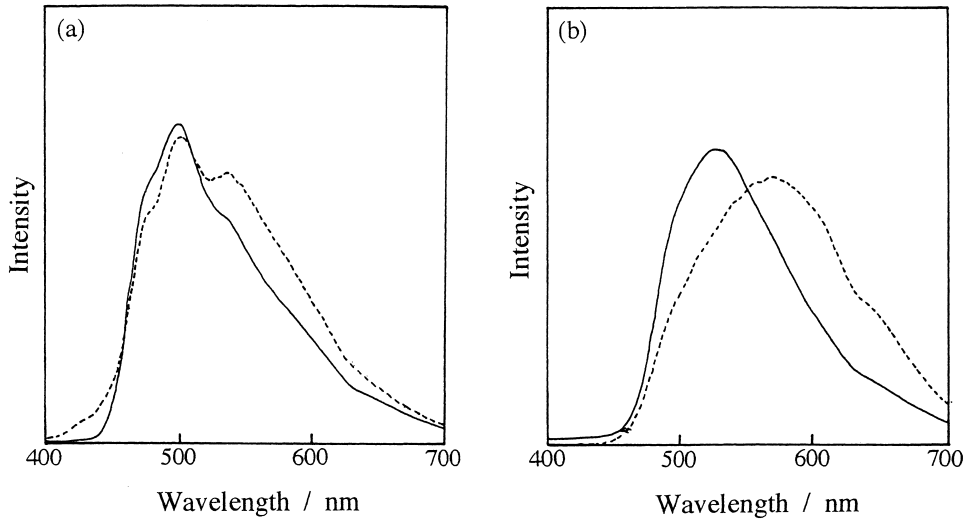

Fig. 7. Solid-state fluorescence spectra of **1** (a) and **2** (b): (- - - -) the original crystal; (——) the solid prepared by slow cooling after heating to 150 °C. λ_{ex} = 360 nm.

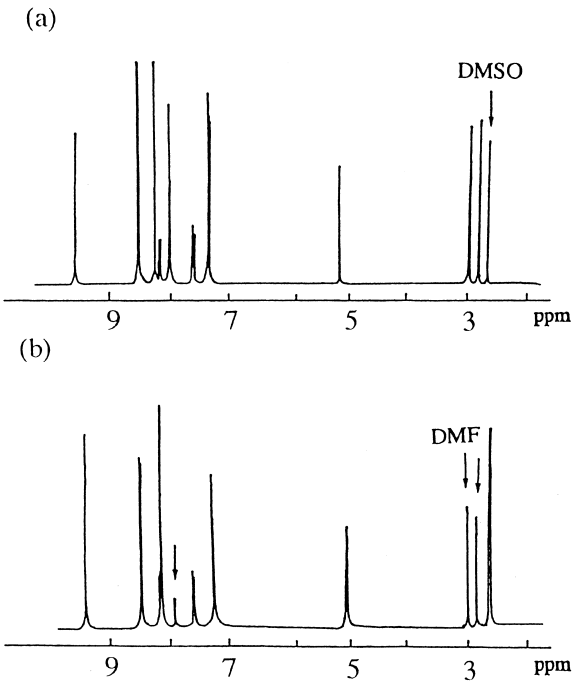

Fig. 8. ^{1}H NMR spectra of **1** (a) in DMF-d_7 and **2** (b) in DMSO-d_6.

assemblies **2** seems to afford an opportunity to create enough space for the inclusion of the DMF molecules (Scheme 1). As shown in Scheme 1, the DMF molecules included in **2** may be surrounded by the anthracene rings of DCA, although details of the exact location of the DMF molecules in the voids remain unclear.

To utilize the assemblies as nanoporous materials with accessible voids, we examined the possibility of removing the solvent molecules from the assembly crystals. The removal of the DMF molecules from **2** was not achieved in vacuum at room temperature. Instead, the DMF molecules can be removed by heating. The DSC curve (first scan) of **2** exhibited a broad endothermic peak in the range of 130–150 °C, which disappeared in the second scan (Fig. 9). Moreover, when **2** was heated up to 150 °C, the signals of DMF disappeared in the ^{1}H NMR spectrum of **2**. These results indicate that the removal of the guest DMF molecules from the crystal of **2** occurs above 130 °C. The FT-IR spectra of **2** did not change by heating. On the other hand, the XRD patterns of **2** prepared by slow cooling after heating to 150 °C clearly indicated the loss of crystallinity. In addition, the peak with Bragg spacing of 14.02 Å, which is indicative of the hexagonal packing, diminished in intensity compared to the original intensity (Fig. 5), suggesting that some deformation of hexagonal packing occurs. This structural deformation also brought about the shift to lower wavelength of the emission in the solid-state fluorescence spectrum of **2** (Fig. 7). Thus, the included DMF molecules play an important role in the stability of the hexagonal packing of the assemblies **2**. Unfortunately, the removal of the included DMF molecules while still maintaining the hexagonal packing has not get accomplished.

No signal of DMSO was observed in the ^{1}H NMR spectrum of **1** heated up to 150 °C, suggesting that the DMSO molecules are also removed from **1** due to heating. The loss of crystallinity and the fluorescence change (the disappearance of the excimer emission) were again observed for **1** prepared by slow cooling after heating to 150 °C. In the DSC second scan of **1**, the endothermic peak observed at 128 °C in the first scan shifted to 121 °C and the peak area decreased to 61% of that observed in the first scan. Moreover, the third scan of **1** also exhibited the endothermic peak at 121 °C. Primrose et al. have reported that tris(*o*-phenylenedioxy)phosphazene had a phase transition from a pure monoclinic phase to a mixed monoclinic/hexagonal type structure.[10] From these observations, a structural transformation due to thermal agitation seems to take place at 128 °C together with the removal of the DMSO molecules from **1** and the structural transformation occurs at 121 °C after the removal of the DMSO molecules from **1**, although details of the transformed structure are unclear.

In the second scans of **1** and **2**, the exothermic process oc-

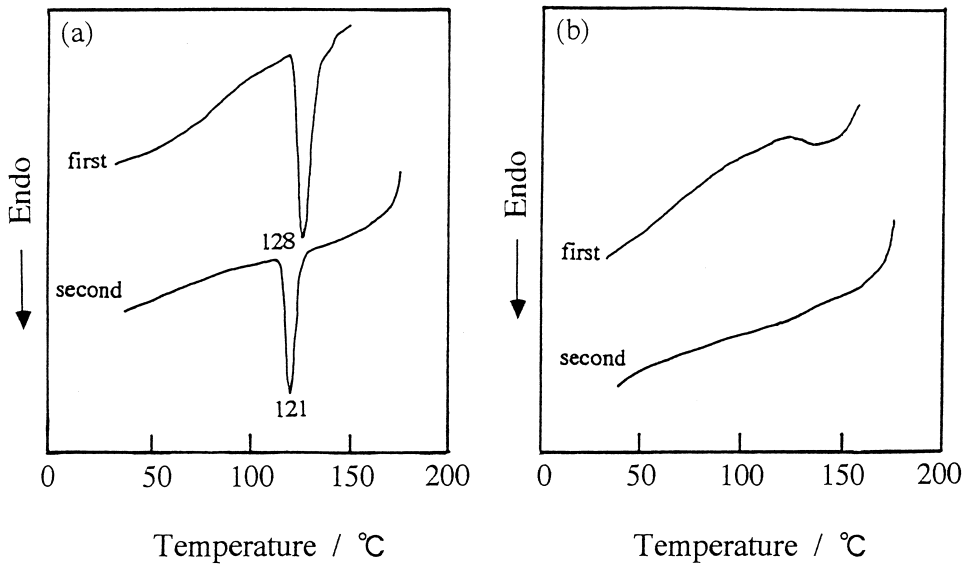

Fig. 9. DSC heating curves of **1** (a) and **2** (b).

curs at ca. 170 °C, indicating the decomposition of the assemblies. Such a temperature is higher than the decomposition temperature of PyPN (100 °C). In addition, the melting of PyPN, which is observed at 75 °C for the pure PyPN, is not visible in the DSC curves, suggesting that PyPN becomes thermally stable in the assemblies. As no endothermic peak due to the hydrogen bond scission was observed in the DSC curves, we conclude that the decomposition of assemblies may arise from the pyrolysis of PyPN in the assembly rather than from the scission of the hydrogen bond.

Conclusions

Two supramolecular self-assemblies, **1** and **2**, were obtained as brown crystals from DMSO or DMF solution containing PyPN and DCA, respectively. The structure of **1**, which is a assembly composed of $[PyPN{\cdot}2(DCA)]_n$, was determined by the single crystal X-ray analysis. On the other hand, the composition of **2** was $[PyPN{\cdot}3(DCA)]_n$. The X-ray diffraction data suggested that the assemblies **2** with cylindrical structure are organized into a hexagonal arrangement. The hexagonal packing of cylindrical assemblies containing bulky and rigid anthracene rings affords effective voids in the crystal, leading to the inclusion of DMF molecules. However, unfortunately, the attempted removal of the solvent molecules and insertion of organic compounds were unsuccessful. Now, we are striving to design supramolecular solids based on cyclotriphosphazene which are capable of reversible binding of guests.

References

1 K. Kato and J. M. J. Frechet, *J. Am. Chem. Soc.*, **111**, 8533 (1989).

2 D. B. Ambabilino and J. F. Stoddart, *Chem. Rev.*, **95**, 2725 (1995).

3 W. A. Herrmann, N. W. Huber, and O. Runte, *Angew. Chem., Int. Ed. Engl.*, **34**, 2187 (1995).

4 L. R. MacGillivray and J. L. Atwood, *Nature*, **389**, 469 (1997).

5 Y. Aoyama, K. Endo, T. Anzai, Y. Yamaguchi, T. Sawaki, K. Kobayashi, N. Kanehisa, H. Hashimoto, Y. Kai, and H. Masuda, *J. Am. Chem. Soc.*, **118**, 5562 (1996).

6 L. Halian, E. D. Charles, L. G. Thomas, G. K. Douglas, and O. M. Yaghi, *J. Am. Chem. Soc.*, **120**, 2186 (1998).

7 S. Kitagawa and M. Kondo, *Bull. Chem. Soc. Jpn.*, **71**, 1739 (1998).

8 S. S.-Y. Chui, S. M.-F. Lo, J. P. H. Charant, A. G. Orpen, and I. D. Williams, *Science*, **283**, 1148 (1999).

9 H. R. Allcock, *Acc. Chem. Res.*, **11**, 81 (1978).

10 A. P. Primrose, M. Parvez, and H. R. Allcock, *Macromolecules*, **30**, 670 (1997).

11 W. Marsh, and J. Trotter, *J. Chem. Soc. A*, **1971**, 169.

12 G. Bandoli, U. Casellato, M. Grassi, E. Montoneri, and G. C. Pappalarde, *J. Chem. Soc., Dalton Trans.*, **1989** 757.

13 K. Inoue, T. Itaya, and N. Azuma, *Supramol. Sci.*, **5**, 163 (1998).

14 T. Itaya, N. Azuma, and K. Inoue, *Supramol. Chem.*, **9**, 121 (1998).

15 T. Itaya and K. Inoue, *Bull. Chem. Soc. Jpn.*, **73**, 2829 (2000).

16 R. O. Garay, H. Naarmann, and K. Mullen, *Macromolecules*, **27**, 1922 (1994).

17 C. J. Gilmore, *J. Appl. Cryst allogr.*, **17**, 42 (1984).

18 M. C. Etter, *Phys. Chem.*, **95**, 4601 (1991).

19 H. Bouas-Laurent, A. Castellan, M. Daney, J.-P. Desvergne, G. Guinand, P. Marsau, and M.-H. Riffaud, *J. Am. Chem. Soc.*, **108**, 315 (1986).